

High-resolution three-dimensional imaging of large specimens with light sheet-based microscopy

Peter J Verveer^{1,3}, Jim Swoger^{1,3},
Francesco Pampaloni¹, Klaus Greger¹,
Marco Marcello² & Ernst H K Stelzer¹

We report that single (or selective) plane illumination microscopy (SPIM), combined with a new deconvolution algorithm, provides a three-dimensional spatial resolution exceeding that of confocal fluorescence microscopy in large samples. We demonstrate this by imaging large living multicellular specimens obtained in a three-dimensional cell culture. The ability to rapidly image large samples at high resolution with minimal photodamage provides new opportunities especially for the study of subcellular processes in large living specimens.

Light sheet-based microscopy, such as SPIM is a new method for imaging large fluorescent samples¹. To achieve optical sectioning, the sample is illuminated with a sheet of light, an approach that has also been applied for macroscopic imaging². The fluorescence is observed with a wide-field microscope, and a charge-coupled device (CCD) camera is used to rapidly acquire images with a high dynamic range. Only the plane that is in focus is illuminated, limiting photodamage and thereby facilitating the acquisition of many planes in large samples. Three-dimensional imaging is achieved by translating the sample along the optical axis of the detection system. The sample is embedded in a cylinder of agarose gel that is mounted in the instrument from above^{3,4}. The gel consists of 0.5–1% agarose in a medium suitable for living specimens, allowing observation for extended periods. This arrangement allows the specimen to be physically turned perpendicular to the optical detection axis, to acquire stacks of images at several fixed rotation angles. These independent views along different directions through the specimen can be merged into a single three-dimensional image with superior isotropic resolution⁵. Moreover, artifacts arising from absorption and scattering within the sample are suppressed.

Here we report the ability of SPIM to acquire three-dimensional images in large living samples with a resolution exceeding that of a

fluorescence confocal microscope. This is achieved by using a reconstruction algorithm that performs a joint deconvolution of data acquired along multiple directions. Deconvolution algorithms use *a priori* knowledge of the optical properties of the microscope that are defined by the point-spread-function (PSF; the image of a single point) to improve spatial resolution^{6,7}. They are commonly applied to widefield fluorescence microscopy data in applications where photodamage and acquisition times are limiting factors and confocal imaging is not viable. The lack of optical sectioning, however, causes artifacts, and spatial resolution is generally inferior to that of confocal imaging. With confocal microscopy only modest improvements are achieved by deconvolution owing to the lower signal-to-noise ratios of the data. SPIM combines the advantageous elements of widefield and optical-sectioning microscopy: data are acquired at high signal-to-noise ratios and with low photodamage, whereas high isotropic resolution is provided by single-plane illumination and by acquisition along multiple directions. For these reasons, SPIM data are particularly well suited for deconvolution approaches.

We designed an algorithm derived from a multiview deconvolution method originally developed to combine images acquired with widefield and confocal modes of fluorescence microscopy⁸ (see **Supplementary Methods** online). To investigate what spatial resolution can be achieved, we recorded the autofluorescence of paper mulberry pollen grains with SPIM and confocal fluorescence microscopy (**Fig. 1**). We present individual slices through the image stacks oriented parallel to the optical detection axis. This highlights differences in resolution along the axial and lateral directions and shows the imaging performance over the entire depth of the specimen. It is evident that the axial resolution of the raw SPIM data is poorer than that of the raw confocal fluorescence microscopy data (**Fig. 1a**), although the latter also does not have isotropic resolution. A weighted spectral averaging SPIM reconstruction⁵ clearly resolves the spherical shell surrounding the core (**Fig. 1b**), but the image appears blurred compared to the confocal data. The SPIM deconvolution, however, yielded higher, more isotropic, resolution compared to the deconvolution of the confocal data (**Fig. 1b**), despite the much lower numerical aperture (NA) of the objective used (NA = 0.9 versus NA = 1.4). Line plots through the shell of the pollen grains (**Fig. 1c**) show that the raw confocal data have a better resolution than the raw SPIM data and the weighted spectral averaging reconstruction. The SPIM deconvolution, however, clearly resolves the shell better than the confocal result along the axial direction (0.4 μm versus 0.7 μm full-width at half-maximum of the peaks).

The data of the pollen grain represent an ideal case where we recorded data along many directions. This is not always feasible

¹Cell Biology & Biophysics Unit, European Molecular Biology Laboratory, Meyerhofstrasse 1, 69117 Heidelberg, Germany. ²Biomedical Structure Group, German Cancer Research Center, Im Neuenheimer Feld 280, 69120, Heidelberg, Germany. ³Present addresses: Department of Systemic Cell Biology, Max Planck Institute of Molecular Physiology, Otto-Hahn-Strasse 11, 44227, Dortmund, Germany (P.J.V.) and Systems Biology Programme, Centre for Genomic Regulation, C/Dr. Aiguader 88, 08003 Barcelona, Spain (J.S.). Correspondence should be addressed to P.J.V. (verveer@mpi-dortmund.mpg.de), J.S. (jim.swoger@crg.es) or E.H.K.S. (stelzer@embl.de).

RECEIVED 13 NOVEMBER 2006; ACCEPTED 18 JANUARY 2007; PUBLISHED ONLINE 4 MARCH 2007; DOI:10.1038/NMETH1017

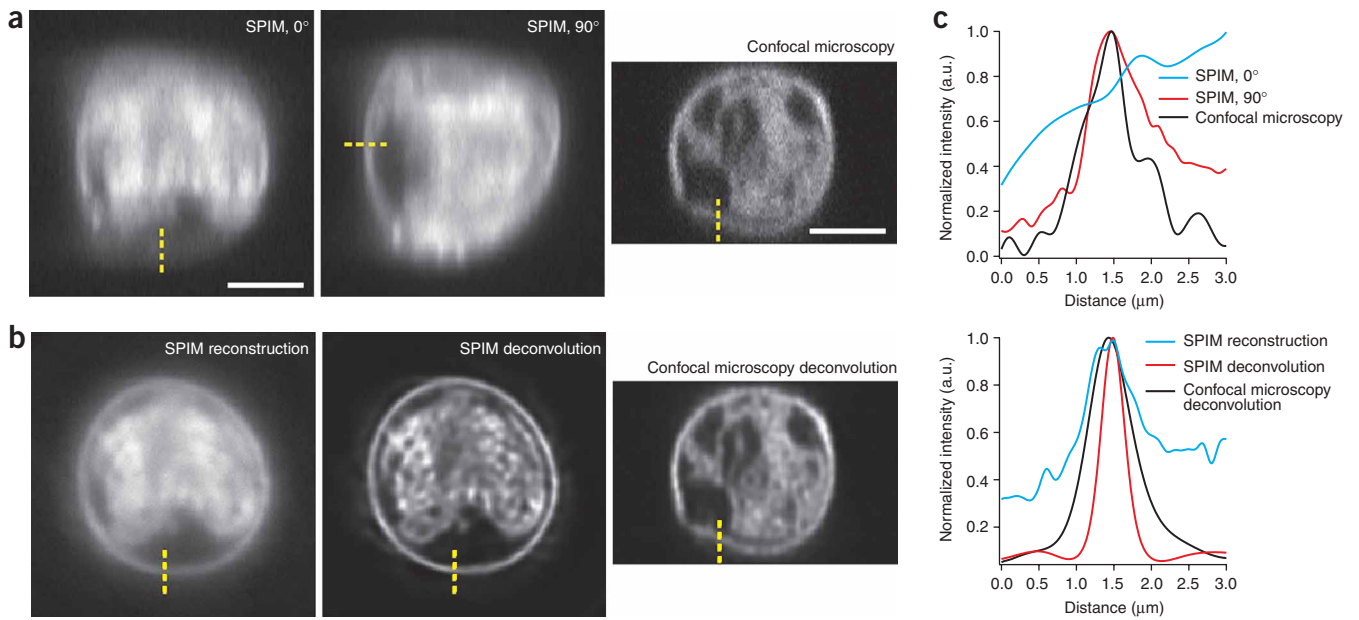


Figure 1 | Comparison of SPIM and confocal fluorescence microscopy by imaging the autofluorescence of grains of paper mulberry pollen. **(a)** Two orthogonal SPIM data sets of the same pollen grain, (obtained by physically rotating the sample perpendicular to the optical axis), and a confocal data set of a similar grain. Images are slices through the three-dimensional stacks parallel to the optical detection axis. Scale bars, 5 μm . **(b)** Weighted spectral averaging reconstruction of SPIM data, deconvolved SPIM data and deconvolved confocal data. **(c)** Intensity plots through the indicated lines.

owing to the use of organic dyes or fluorescence proteins that are easily photobleached. Moreover, acquisition times may be limited in living samples. We were able to image single cells expressing protein fusions with a resolution comparable to that of fluorescence confocal microscopy using a limited number of SPIM stacks (Supplementary Fig. 1 online). One of the strengths of SPIM is its ability to image large living specimens. Our approach is indeed beneficial for very large samples acquired using low-NA lenses (Supplementary Fig. 2 online), but we are especially interested in imaging large living samples with high subcellular resolution. We therefore imaged Madin-Darby canine kidney (MDCK) cells, which form hollow cysts consisting of a monolayer of cells when grown in a collagen gel³. We stably transfected these cells with a gene encoding GFP-tagged actin and labeled nuclear DNA with DRAQ5. The weighted spectral averaging SPIM reconstruction clearly shows the outlines of individual cells by the GFP-actin localization, whereas the confocal data are noisier and exhibit artifacts as a result of light absorption, scattering and photobleaching in the upper and lower parts of the cyst (Fig. 2a). Deconvolution (Fig. 2b) yields a much-improved result for the SPIM data with high isotropic resolution. Deconvolution of the confocal data, however, shows substantial artifacts in the upper and the lower parts of the cyst, and resolution is poorer in the axial direction. Moreover, the deconvolution procedure removed the GFP-actin signal inside the cells, most likely because the signal-to-noise ratio of the data in these regions was too poor. Thus, the deconvolved SPIM data revealed details in the sample more accurately than the deconvolved confocal data despite the considerably lower NA of the objective used (SPIM, NA = 0.8; confocal microscopy, NA = 1.2).

These samples were fairly large (~35 μm diameter), but they could in principle be imaged by confocal microscopy, although the results were suboptimal compared to those obtained by SPIM. We

therefore imaged a large cellular spheroid of BxPC3 human pancreatic cancer cells (~140 μm diameter) stained with DRAQ5 (Fig. 3). This type of spheroid has been successfully used as a model for tumor angiogenesis⁹ and for high-throughput screening for new anti-tumor drugs¹⁰. Confocal microscopy of

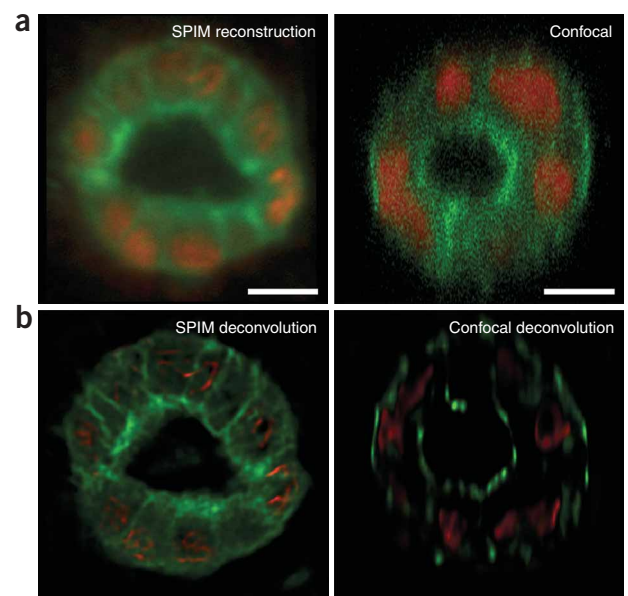


Figure 2 | Comparison of SPIM and confocal fluorescence microscopy of MDCK cysts. **(a)** The MDCK cells were stably expressing GFP-actin (green) and labeled with DRAQ5 (red). Weighted spectral averaging reconstruction of SPIM data and fluorescence confocal microscopy data. Images are slices through the three-dimensional stacks parallel to the optical detection axis. Scale bars, 10 μm . **(b)** Deconvolution results for SPIM and confocal data.

the same sample was not feasible (see **Supplementary Fig. 3** online), but with SPIM we obtained high-resolution images showing clearly resolved nuclear structures. The slice shown is oriented parallel to the detection axis, demonstrating that high resolution is obtained throughout the full depth of this large sample. From our combined results we conclude that for large living samples, SPIM with deconvolution provides superior imaging with high spatial resolution compared to confocal imaging.

With large samples such as those demonstrated here, specimen-induced aberrations need to be taken into account. The SPIM data are less susceptible to such artifacts than confocal microscopy data (see **Figs. 2, 3**, and **Supplementary Fig. 3**), and good results can be obtained. Nevertheless, future work should include corrections for specimen-induced aberrations to further improve spatial resolution¹¹.

Without deconvolution SPIM provides a higher spatial resolution than fluorescence confocal microscopy when low-NA objectives ($NA < 0.8$) are used, whereas it is expected to outperform widefield and two-photon microscopy even with high-NA objectives¹². Our results show that with deconvolution, SPIM with medium NAs (0.8–0.9) is also capable of outperforming confocal microscopy at high NAs (1.2–1.4). For imaging single cells growing on coverslips, various fluorescence techniques are emerging that are capable of providing a higher spatial resolution¹³, but these approaches are not suitable for large samples. For large living specimens, such as whole organisms or multicellular specimens produced by three-dimensional cell culture, the advantages of SPIM in terms of minimizing photodamage and fast acquisition speed have been demonstrated before¹. Our results now show that, in addition to these strengths, SPIM also allows imaging with high spatial resolution. SPIM therefore opens up new opportunities for studying subcellular processes in the context of large living specimens.

Note: Supplementary information is available on the Nature Methods website.

ACKNOWLEDGMENTS

We thank D. Holzer (European Molecular Biology Laboratory, Heidelberg) for help with MDCK cell culture and transfection, and A. Schrödel and M. Löhner (German

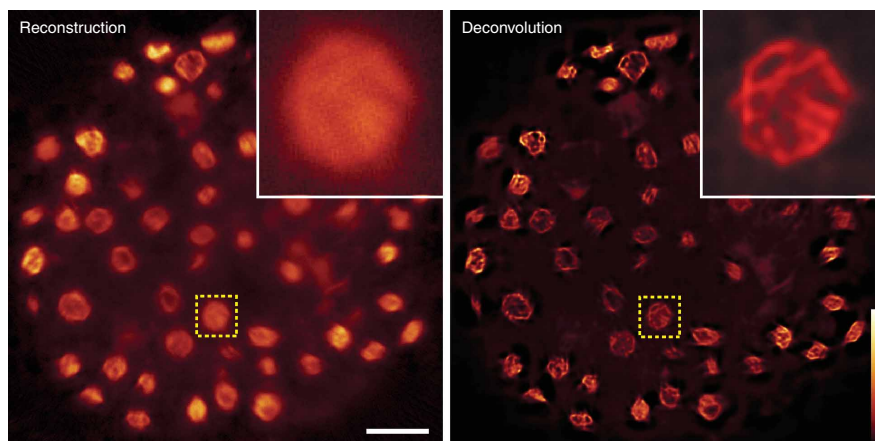


Figure 3 | Images recorded using SPIM of a large cellular spheroid of BxPC3 human pancreatic cancer cells labeled with DRAQ5. Images are slices through the three-dimensional stacks parallel to the optical detection axis. The insets show magnifications of the indicated regions. Scale bars, 20 μm .

Cancer Research Center, Heidelberg) for providing the BxPC3 spheroids. E.H.K.S. and F.P. acknowledge the Forschungsprogramm Optische Technologien der Landesstiftung Baden-Württemberg for financial support. M.M. was supported by a joint collaboration between Hamamatsu and the German Cancer Research Center (Project PA 11631).

COMPETING INTERESTS STATEMENT

The authors declare no competing financial interests.

Published online at <http://www.nature.com/naturemethods/>
Reprints and permissions information is available online at
<http://npg.nature.com/reprintsandpermissions>

- Huisken, J., Swoger, J., Del Bene, F., Wittbrodt, J. & Stelzer, E.H.K. *Science* **305**, 1007–1009 (2004).
- Voie, A.H., Burns, D.H. & Spelman, F.A. *J. Microsc.* **170**, 229–236 (1993).
- Keller, P.J., Pampaloni, F. & Stelzer, E.H.K. *Curr. Opin. Cell Biol.* **18**, 117–124 (2006).
- Greger, K., Swoger, J. & Stelzer, E.H.K. *Rev. Sci. Instrum.* (in the press).
- Swoger, J., Huisken, J. & Stelzer, E.H.K. *Opt. Lett.* **28**, 1654–1656 (2003).
- Agard, D.A. & Sedat, J.W. *Nature* **302**, 676–681 (1983).
- Carrington, W.A. *et al. Science* **268**, 1483–1487 (1995).
- Verveer, P.J. & Jovin, T.M. *Appl. Opt.* **37**, 6240–6246 (1998).
- Timmins, N.E., Dietmair, S. & Nielsen, L.K. *Angiogenesis* **7**, 97–103 (2004).
- Kunz-Schughart, L.A., Freyer, J.P., Hofstaedter, F. & Ebner, R. *J. Biomol. Screen.* **9**, 273–285 (2004).
- Kam, Z., Hanser, B., Gustafsson, M.G., Agard, D.A. & Sedat, J.W. *Proc. Natl. Acad. Sci. USA* **98**, 3790–3795 (2001).
- Engelbrecht, C.J. & Stelzer, E.H.K. *Opt. Lett.* **31**, 1477–1479 (2006).
- Hell, S.W. *Nat. Biotechnol.* **21**, 1347–1355 (2003).